# Suppression of Ni agglomeration in PLD fabricated Ni-YSZ composite for surface modification of SOFC anode

Ho-Sung Noh [a,b], Ji-Won Son [a,*], Heon Lee [b], Ho-Il Ji [a], Jong-Ho Lee [a], Hae-Weon Lee [a]

[a] *High-Temperature Energy Materials Center, Korea Institute of Science and Technology, Seoul 130-650, Republic of Korea*
[b] *Department of Materials Science and Engineering, Korea University, Seoul 136-701, Republic of Korea*

## Abstract

The suppression of Ni agglomeration in Ni-yttria stabilized zirconia (Ni-YSZ) nano-composite thin films deposited by pulsed laser deposition (PLD) has been investigated by varying post-annealing temperatures at a range of 800–1200 °C. Grain growth to a certain extent appears to be necessary to obtain a stable Ni-YSZ composite microstructure by suppressing massive Ni agglomeration. The microstructurally stable and uniform nano-porous Ni-YSZ thin film was obtained by 1200 °C post-annealing and reduction of the NiO–YSZ thin film, and it was applied as the surface modification layer of the bulk anode support used in conventional solid oxide fuel cells (SOFCs). By this approach, we were able to successfully realize a thin film electrolyte SOFC exhibiting the open cell voltage (OCV) higher than 1 V with a 1-$\mu$m thick film electrolyte on the porous anode support.

## 1. Introduction

Solid oxide fuel cells (SOFCs) increasingly draw much attention as potential candidates for next generation portable and mobile power sources because the merits of SOFCs such as high power and energy densities, system efficiencies, and fuel flexibility are also very advantageous properties for portable power sources.[1–8] However, for realizing miniaturized SOFCs for portable applications, it is necessary to lower operating temperature from a conventional operation range ($\geq$800 °C) without performance compromise to cut down the burden in thermal insulation in an integrated power pack.[1,2,4,5]

To lower the operating temperature of SOFCs, employing thin film electrolytes for reducing the ohmic resistance has been studied intensively.[2,4–9] Nevertheless, due to the current constriction,[10,11] nano-structured electrodes should be employed as well for taking advantage of the electrolyte thickness reduction.[1,2,10,11] The current constriction indicates that if the particle size of the electrode is much bigger in dimension than the electrolyte thickness then the electrolyte area will not be effectively utilized; and it was predicted that the electrode particle distance should be on the order of the thickness of the electrolyte to optimize the electrolyte resistance.[10,11] The particle distance is typically 1.5–4 times of the electrode particle size,[11] therefore, for using the electrolyte with a thickness less than 1 $\mu$m, we need to realize the electrode with at most several hundred nanometer size grains. Thus, both thin electrolytes and nano-structured electrodes should be employed in realizing thin film electrolyte micro-SOFCs.[1,10]

To obtain nano-structured electrodes for thin electrolytes, most of thin film base SOFCs use single phase noble metal electrodes such as porous Pt fabricated by sputtering,[4,6,8,10,12] but the metal coarsening at operating temperatures eventually leads to serious problems such as the reduction of the triple phase boundary length and thus degradation of the cell performance.[10,12] Therefore, ceramic–metal composites (cermets) fabricated by thin film deposition methods[1,13–22] were investigated actively to prevent the metal coarsening since the ceramic network in the nano-composite is expected to retain the excessive metal grain growth[6,23] as in conventional SOFCs. In some cases, desirable microstructures, such as a nano-porous structure and an interpenetrating nano-composite structure,[19,22] as well as

promising electrochemical performances, such as lower overpotentials and electrode resistances,[20–22] were reported. However, in many cases, even more massive metal phase agglomeration was observed after the reduction or thermal treatments of the thin film composites regardless of the deposition methods,[1,13,15–18] which leads to the loss of the connectivity and the poor high temperature stability of electrodes.

In our previous work on NiO- and Ni-yttria stabilized zirconia (YSZ) fabricated by pulsed laser deposition (PLD),[1] it was found to be extremely challenging to obtain a nano-structured Ni-YSZ composite which is nano-porous and conductive at the same time at a processing temperature lower than 700 °C. A NiO–YSZ thin film which was room temperature deposited and post-annealed at 700 °C developed a porous structure, but electrical conduction was not detected when reduced. On the other hand, 700 °C deposited NiO–YSZ films exhibited electrical conduction after the reduction. However, unbearable massive Ni agglomeration occurred. It was also found that the as-deposited NiO–YSZ film was composed of minute equiaxed crystallites (diameter ∼ several nm), which was postulated to be the origin of the large driving force for the Ni coarsening.[1]

Thus, we could assume that grain growth to a certain level may be effective to suppress Ni coarsening. This assumption is supported by the results reported in a previous work[13] where massive Ni coarsening was suppressed in high temperature annealed ($T_{anneal} = 800$ °C, 1000 °C) NiO-gadolinia doped ceria (GDC) thin films deposited by spray pyrolysis. Spray pyrolysis deposited films, however, have differences in terms of the microstructure from the films deposited by PVD including PLD. Sprayed films have a much more porous microstructure than that of PVD deposited films. This is probably the reason why PLD deposited composite films (40 vol% Ni) showed more severe Ni agglomeration[1] than that was reported in spray pyrolysis fabricated composite films subjected to the harsher reduction condition (at 600 °C for 72 h) and with higher Ni content (60 vol%).[13] There are still many unknown facts in terms of the effect of the post-annealing on the microstructure and properties of the cermet composite in the form of the dense thin film fabricated by PVD.

Therefore, in this study, we investigated the behavior of NiO- and Ni-YSZ nano-composite thin films deposited by PLD as a function of post-annealing temperatures and reduction conditions. Since one of the main purposes of the study is to obtain a microstructurally stable nano-structured Ni-YSZ composite anode for the thin film electrolyte of SOFCs, the above-mentioned variables have been changed to establish the condition for achieving desirable nano-porous structures without Ni agglomeration. The microstructure of the thin film NiO- and Ni-YSZ composite; suppression of Ni agglomeration in Ni-YSZ by post-annealing; and eventually application to the thin (∼1 μm) electrolyte SOFC will be presented.

## 2. Experimental procedure

NiO–YSZ composite thin films were deposited by using PLD. A KrF eximer laser ($\lambda = 248$ nm, COMPEX Pro 201F, Coherent) was used as an ablation source. The laser fluence was ∼2.5 J/cm$^2$

on the target surface and the target-to-substrate distance was kept as 5 cm. The target was fabricated by sintering a NiO–YSZ pellet at 1400 °C for 3 h. The pellets were prepared by uniaxial pressing of the powder mixture of NiO (Sumitomo Metal Mining) and 8YSZ (8 mol% $Y_2O_3$ stabilized $ZrO_2$, TZ-8Y, Tosoh Corp.) with a 56:44 wt% ratio of NiO to YSZ. This composition would render the final Ni vol% after reduction in the solid content to be 40%. As was reported previously,[1] the film deposited by using this target has a composition of an Ni:YSZ molar ratio of 65.1:34.9. This molar ratio corresponds to approximately 37.5 vol% Ni to YSZ, which is not a significant deviation from the intended composition. NiO–YSZ films were deposited at a substrate temperature ($T_s$) of 700 °C and $O_2$ ambient pressure ($P_{O_2\,amb}$) of 6.67 Pa. The as-deposited film is a crystalline composite of NiO–YSZ consisting of 2–3 nm equiaxed grains.[1] Deposition for 1 h yielded about 600 nm thick NiO–YSZ films. Initially, $SiO_2$/Si wafer pieces covered with 1 μm YSZ thin films deposited at $T_s = 700$ °C and $P_{O_2\,amb} = 6.67$ Pa by PLD (denoted as YSZ/$SiO_2$/Si hereafter) were used as substrates to compare the results with the previous study.[1] Preliminary experiments to select the post-annealing temperature range were performed on YSZ/$SiO_2$/Si substrates. Post-annealing was performed in air at 800, 1000, and 1200 °C for 1 h. The reduction for the films deposited on YSZ/$SiO_2$/Si was performed at 500 °C for 1 h in 4% $H_2$ (Ar balance), same as the previous study.[1] By the reduction, the NiO–YSZ films were changed to the Ni-YSZ films.

After the post-annealing temperature range was fixed as $T \geq 1000$ °C, the substrates were changed to conventional, bulk-processed NiO–YSZ anodes. The anode supports were prepared by tape-casting and sintering at 1300 °C for 4 h. The surface of the anode was polished down to 0.25 μm using diamond suspensions for removing macro-defects on the surface. Approximately 2-μm thick NiO–YSZ films were deposited and post-annealing at 1000, 1100, and 1200 °C was performed. Two reduction conditions were experimented. The films were reduced in 4% $H_2$ (Ar balance) at 600 °C for 5 h and at 800 °C for 10 h. The former reduction condition was selected because it is the minimum required condition for reducing bulk NiO–YSZ anode supports, and the latter reduction condition was selected to raise the temperature to the operation temperature of conventional SOFCs and to increase the degree of reduction. The surface and cross-sectional microstructures of the films were characterized by using scanning electron microscopy (SEM, XL-30 FEG and NOVA NanoSEM200, FEI). For a material distribution analysis in selected specimens, a dual beam-focused ion beam (FIB) apparatus and back-scattered electron (BSE) images were utilized (Nova 600, FEI).

After the optimization of the conditions for realizing Ni-YSZ nano-composites without Ni agglomeration, the applicability of nano-composites for surface modification of the SOFC anode to obtain a functioning thin film (∼1 μm) electrolyte was investigated by fabricating 2 cm × 2 cm SOFC stamp cells. The layer of the PLD fabricated nano-composite will be denoted as an 'interlayer' hereafter, because the nano-composite layer resides between the bulk anode support and the thin film electrolyte. Tape casted NiO–YSZ sintered at 1300 °C for 4 h was used as

the anode support for the cell fabrication as well. NiO–YSZ nano-composites were formed over the anode support then a 1-$\mu$m thick YSZ layer was deposited at $T_s = 700\,°C$, $P_{O_2\,amb} = 6.67\,Pa$ by PLD. Cathodes were also fabricated by using PLD. For comparison, we fabricated and characterized a cell with a 1 $\mu$m thick YSZ layer directly deposited on the anode support without the interlayer. A detailed cell testing configuration is described elsewhere.[24] OCV developments during the reduction were monitored by using an Iviumstat electrochemical analyzer (Iviumstat, Ivium Technologies).

## 3. Results and discussion

We reported in the previous work that due to the extremely small crystallite size (a few nm) of the PLD as-deposited ($T_s = 700\,°C$) NiO–YSZ film, the driving force for Ni coarsening was extremely high and thus over-sized Ni agglomerates were generated.[1] Therefore, it appears that grain growth to a certain level is necessary to obtain a Ni-YSZ anode without Ni agglomeration, which is microstructurally stable and nano-porous at the same time. In other reports,[13,15] it was also observed that post thermal treatments mitigated Ni agglomeration, which supports that the necessity of the grain growth.

In Fig. 1(a) and (b), the surface morphologies of Ni-YSZ films on YSZ/SiO$_2$/Si substrates obtained by the reduction of post-annealed NiO–YSZ films are displayed. The post-annealing temperatures were 800 and 1000 °C for Fig. 1(a) and (b), respectively, and the reduction was performed at 500 °C for 1 h in 4% H$_2$ (Ar balance). Compared with the film which was obtained by reducing NiO–YSZ as-deposited film ($T_s = 700\,°C$) at the same reduction condition shown in Fig. 1(c),[1] the extent of the Ni agglomeration is very much reduced by the subsequent post-annealing. However, as shown in Fig. 1(a), scattered Ni agglomerates in 800 °C annealed specimen were still observed, which indicates that the complete suppression of the massive Ni agglomeration in 800 °C annealed film was not possible. On the other hand, 1000 °C annealed specimens did not show the Ni agglomeration at this reduction condition and a fine porous structure was obtained as shown in Fig. 1(b). No Ni agglomeration was observed in 1200 °C annealed specimen either, so for further experiments the post-annealing temperature was determined to be $\geq 1000\,°C$.

After confirming the possibility of suppressing Ni coarsening by post-annealing in the films deposited on YSZ/SiO$_2$/Si, we performed further investigation on Ni- and NiO–YSZ composite films by using sintered bulk NiO–YSZ anode supports as substrates. To induce the grain growth in NiO–YSZ composite (40 vol% Ni) films deposited at 700 °C on the anode supports, post-annealing was performed at 1000, 1100, and 1200 °C. In Fig. 2, the surface and cross-sectional microstructures of NiO–YSZ composite thin films annealed at 1000, 1100, and 1200 °C for 1 h are shown. The average grain diameters are $51.8 \pm 3.6$, $93.0 \pm 7.5$, and $177.9 \pm 15.5$ nm in 1000, 1100, and 1200 °C annealed specimens, respectively. The grain sizes were measured by the line intercept method in the top-view micrographs with an enhanced contrast which were taken at various magnifications and then by applying shape factor of 1.5,
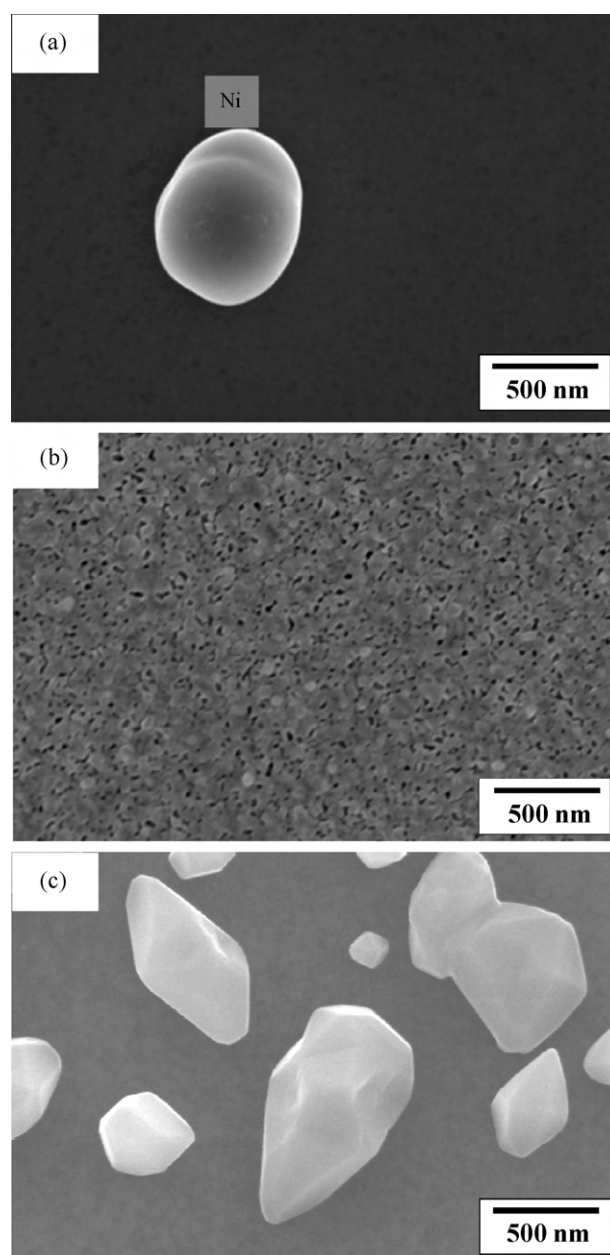


Fig. 1. Surface morphologies of Ni-YSZ (Ni 40 vol%) films on YSZ/SiO$_2$/Si substrates obtained after post-annealing at (a) 800 °C and (b) 1000 °C for 1 h in air then reduced at 500 °C for 1 h in 4% H$_2$ (Ar balance). (c) The surface morphology of Ni-YSZ (Ni 40 vol%) film which is obtained by reducing non-post-annealed film deposited at 700 °C[1].

roughly assuming spherical grains.[25] In cross-sectional micrographs displayed in Fig. 2(b), (d) and (f), it is shown well that approximately 2-$\mu$m thick dense thin film NiO–YSZ layers are formed over micron-scale grains of the anode supports.

In Fig. 3(a)–(f), the microstructures of Ni-YSZ films which are obtained by the reduction of post-annealed NiO–YSZ films are displayed. The reduction was performed at 600 °C for 5 h in 4% H$_2$. Films annealed at $T \geq 1000\,°C$ did not exhibit the Ni agglomeration even though these were exposed to a harsher reduction condition than that (500 °C for 1 h) applied to the films that were not post-annealed.[1] For excluding the possi-
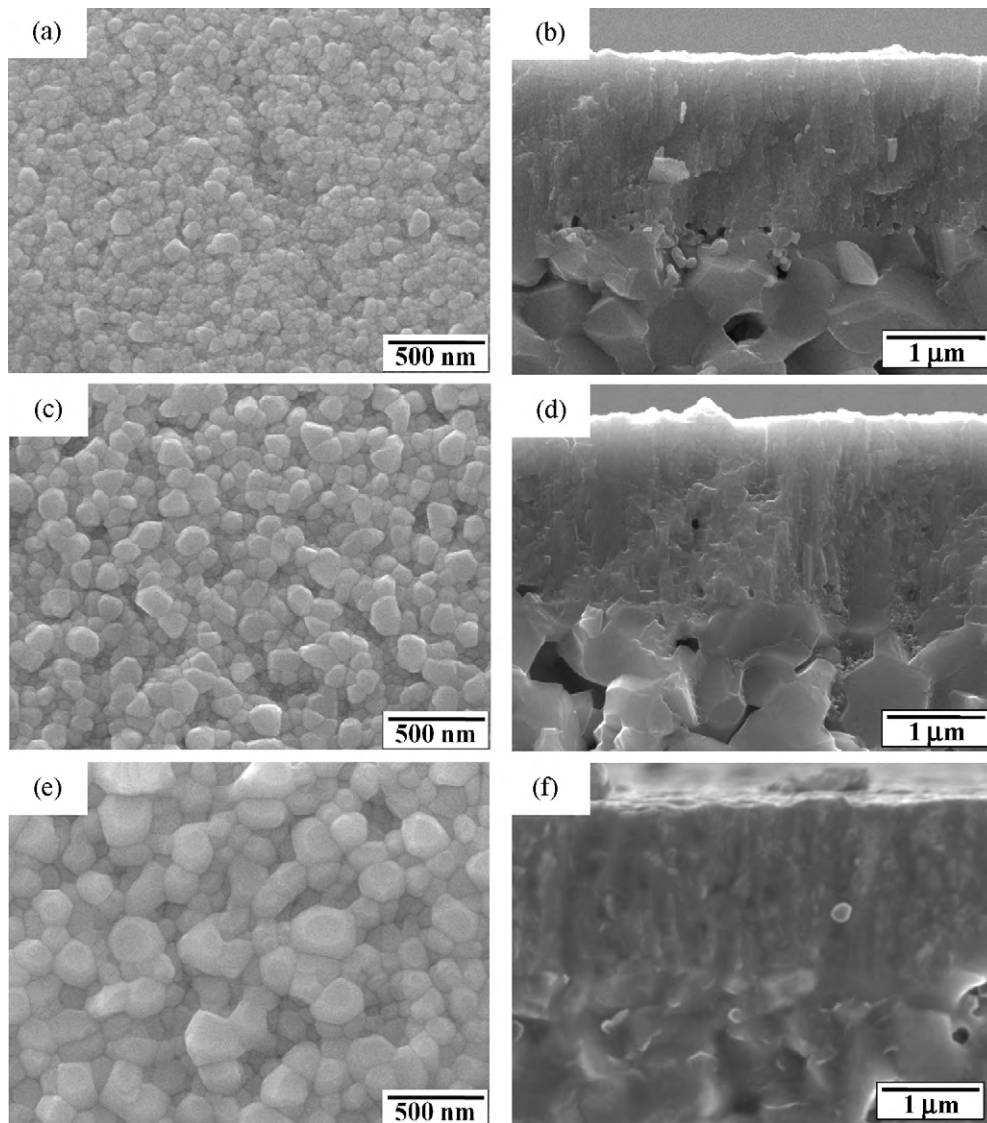
Fig. 2. SEM micrographs of surfaces and cross-sections of NiO–YSZ (Ni 40 vol%) films post-annealed at (a), (b) 1000 °C; (c), (d) 1100 °C; (e), (f) 1200 °C for 1 h.

bility that the difference originates from the substrate change, the reduced microstructures (at 500 °C for 1 h) of the film on the anode support which was not post-annealed are shown in Fig. 3(g) and (h). It is clearly shown that also on the anode support, the massive Ni agglomeration is unavoidable in the film that was not post-annealed. On the contrary, the films post-annealed at $T \geq 1000$ °C showed fine porous structures without Ni agglomeration at this reduction condition (600 °C, 5 h). In the cross-sectional microstructures (Fig. 3(b), (d), and (f)), it is shown that the microstructural characteristics such as nano-porous structures and equiaxed grain shapes are consistent throughout the thickness of the thin film layer.

To show the material distribution in the Ni-YSZ film layer, a BSE image of the 1200 °C post-annealed and reduced specimen (Fig. 3(f)) is shown in Fig. 4. The specimen was milled with FIB for observation. Ni grains are brighter than YSZ grains due to the atomic contrast. Due to the magnetic property of Ni, it was very challenging to obtain high magnification pictures. The specimens annealed below 1100 °C could not be analyzed well

with SEM because that the minute grain size cannot be discerned at the current resolution so the image of 1200 °C post-annealed specimen in shown only. It is shown well that Ni is homogeneously distributed in the YSZ matrix in the film layer, as similar to in the bulk support shown beneath, only with a much finer scale microstructure.

When the reduction condition becomes more severe, however, the post-annealed composite structure becomes less stable for the specimens annealed at lower temperatures, i.e., films with smaller grain sizes. In Fig. 5, the films that are annealed at 1000, 1100, and 1200 °C then reduced at 800 °C for 10 h are exhibited. To compare the difference in the degree of the Ni agglomeration, lower magnification pictures are provided. It is shown that the Ni agglomeration has occurred in the specimens annealed at 1000 °C and 1100 °C. The microstructure of the specimen annealed at 1200 °C appeared not to exhibit the Ni agglomeration. This observation supports that the driving force for the agglomeration becomes higher for finer Ni grains. It is also surprising that the Ni agglomeration in 1000 °C annealed specimen
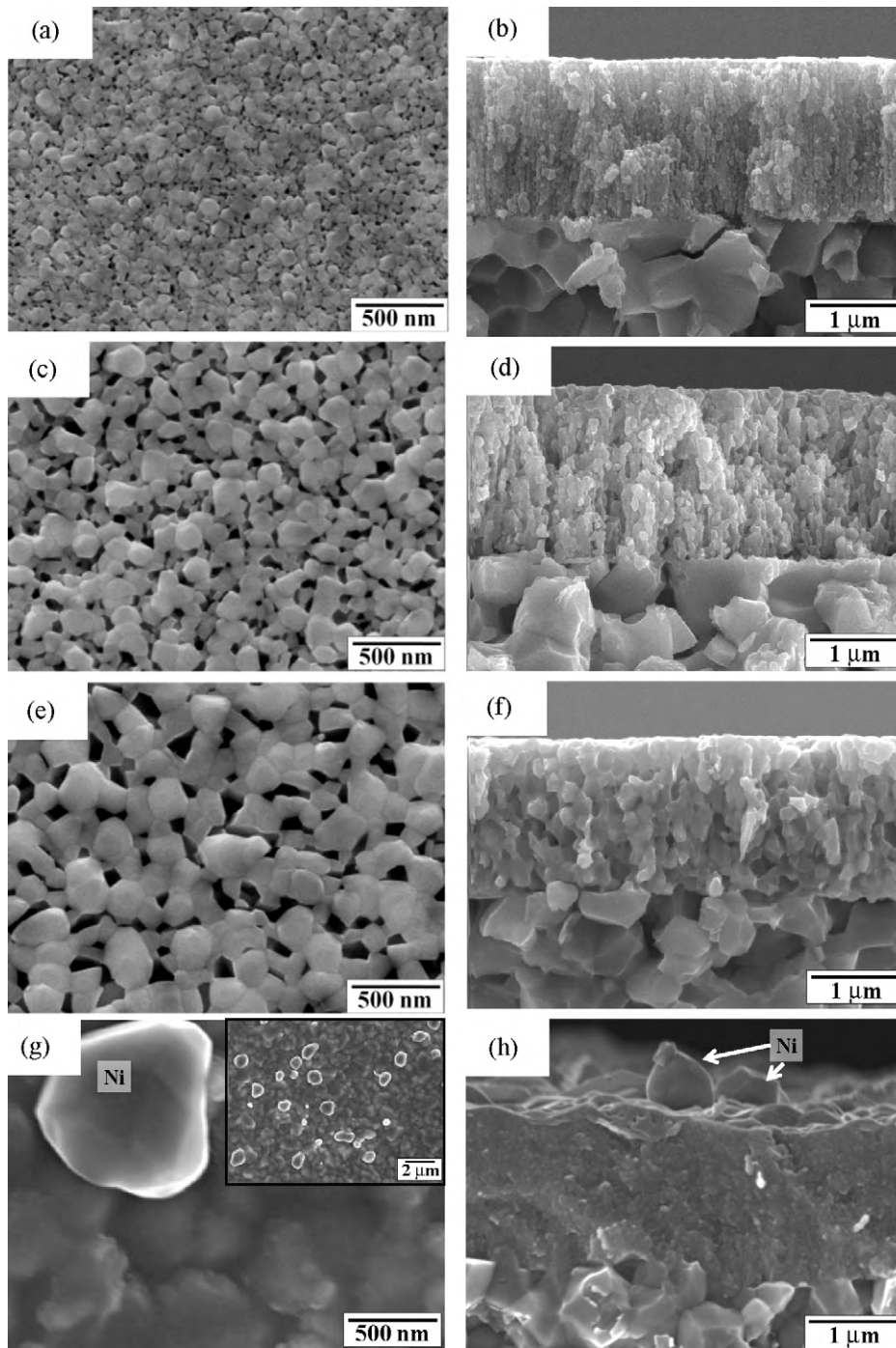
Fig. 3. Reduced (600 °C 5 h in 4% $H_2$) microstructures of NiO–YSZ films annealed at (a), (b) 1000 °C; (c), (d) 1100 °C; (e), (f) 1200 °C for 1 h. (g), (h) reduced (500 °C 1 h in 4% $H_2$) microstructrure of NiO–YSZ films after deposition at 700 °C, without post-annealing (inset of (g) shows lower magnification picture).

is severe enough to tear the film, as shown in Fig. 5(a). In 1100 °C annealed specimen, Ni agglomeration occurred but the size of the agglomerates is much smaller and cracking of the film layer did not appear.

The exact reason why the Ni agglomeration is suppressed through the grain growth by the post-annealing cannot be concluded at the current stage without the solid evidence of the Ni agglomeration mechanism. However, there can be several assumptions. One is that the massive Ni agglomeration occurs

due to the evaporation and condensation of fine Ni grains. If we see Fig. 1(a) and (c), and Fig. 3(g), the Ni agglomerates appears to reside on the surface of the PLD NiO–YSZ layer. The reduction of NiO to Ni should occur on the surface where NiO and $H_2$ meet, and thus Ni nuclei should be formed on the surface of the film.[16] If the gas-phase transport has been involved then the agglomerate will grow on the surface. The driving force of evaporation could be reduced by the grain growth of the NiO/Ni so the post-annealing can be effective to suppress the generation
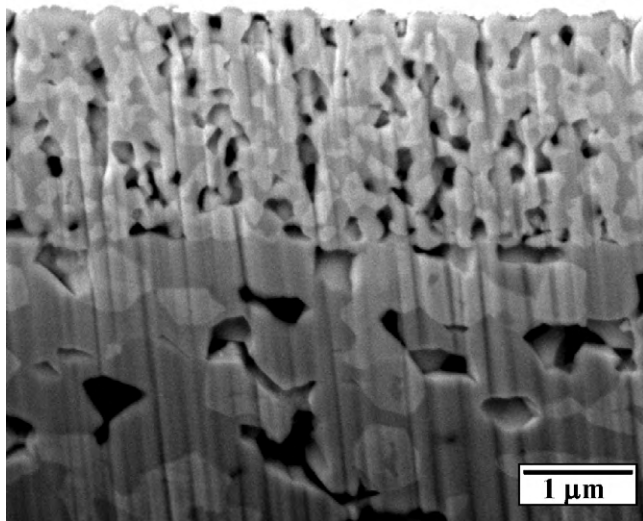
Fig. 4. BSE image of 1200 °C post-annealed and reduced (600 °C 5 h in 4% $H_2$) film.

of over-sized Ni agglomerates. However, if we observe Fig. 5(a), the over-sized Ni agglomerates appears to be squeezed out where the crack generated in the film layer, which cannot be explained by the evaporation and condensation mechanism only. It seems that the massive Ni agglomerates pushed away the film matrix as was postulated by Muecke et al.[13] This implies that the result is related to the strength of the YSZ network also.

Because the functionality of the YSZ in the Ni-YSZ composite is to retain the dispersion of the metal particles and the porosity of the anode,[23] if the three dimensionally connected YSZ network is structurally strong enough then the suppression of the Ni agglomeration should be effective even if the driving force for Ni agglomeration is high. The strength of the YSZ network has a correlation with the post-annealing temperature. Fig. 5(a) shows that the strength of the YSZ network annealed at 1000 °C is not enough to suppress massive Ni agglomeration at a harsher reduction condition, and the network could be destroyed by Ni agglomeration at the 800 °C 10 h reduction condition. It appears that the 1200 °C annealed thin film composite has a low Ni agglomeration driving force due to grain growth as well as a strong YSZ network. Even though we cannot conclude which mechanism is dominant for explaining the phenomena we observe, it is certain that the grain growth and the network strengthening by the post-annealing are effective, or even essential to secure the microstructural stability of the Ni-YSZ cermet anode fabricated by PLD.

These results imply that nano-structured cermet composites may have a restriction in terms of the operating temperature range and duration depending on the microstructures determined by the post-annealing temperature, which could be detrimental to the stability at high temperature applications such as conventional SOFCs. But still, 1000 and 1100 °C post-annealed nano-composites exhibited microstructural stability at a low temperature (~600 °C). Therefore, we postulate that the nano-composites with grain growth to several tens of nanometer could be employed for the operations at temperatures ≤ ~500–600 °C which is the operation temperature range of micro-SOFCs.[5]
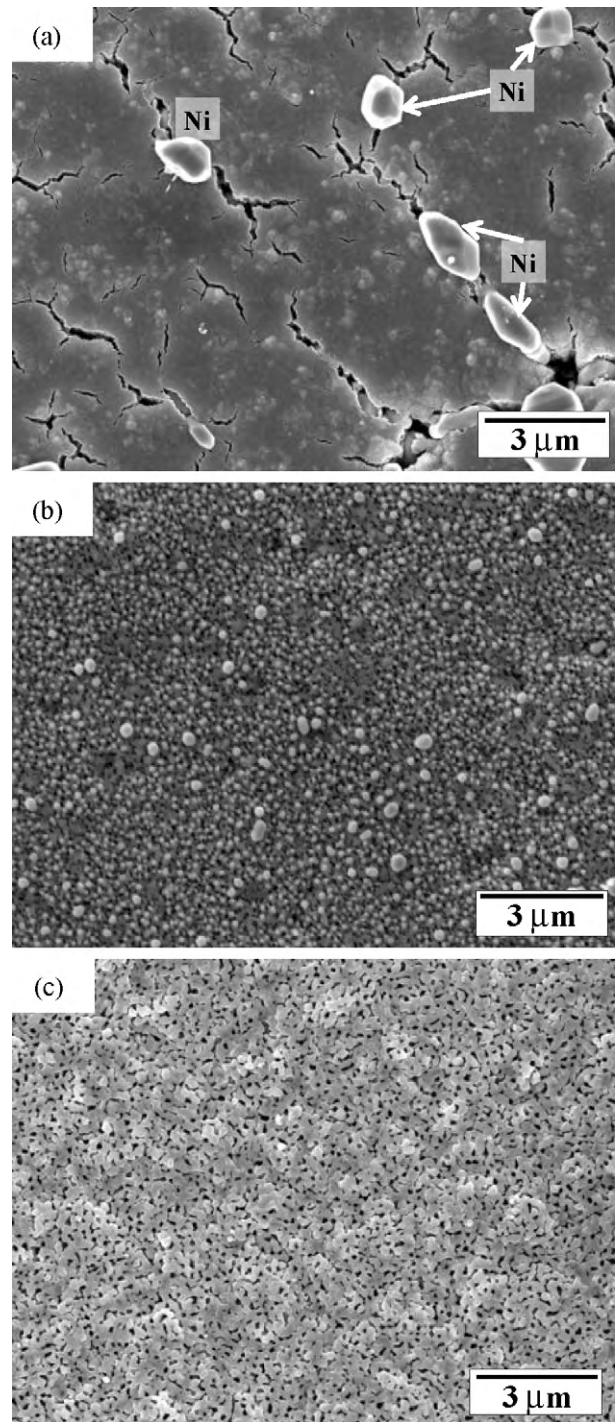


Fig. 5. Surface morphologies of NiO–YSZ films annealed at (a) 1000 °C, (b) 1100 °C, and (c) 1200 °C after reductions at 800 °C 10 h.

However, long-term stability at this temperature range should be studied further. For higher temperature and longer lasting operations, we think that the grain size should be in the range of hundreds nanometers, which requires high temperature post-annealing at $T \geq 1200$ °C.

Given that the post-annealing is essential to suppress the massive Ni agglomeration and to attain the YSZ network strength, it is thought that it would be extremely challenging to fabricate a microstructurally stable composite cermet anode after a
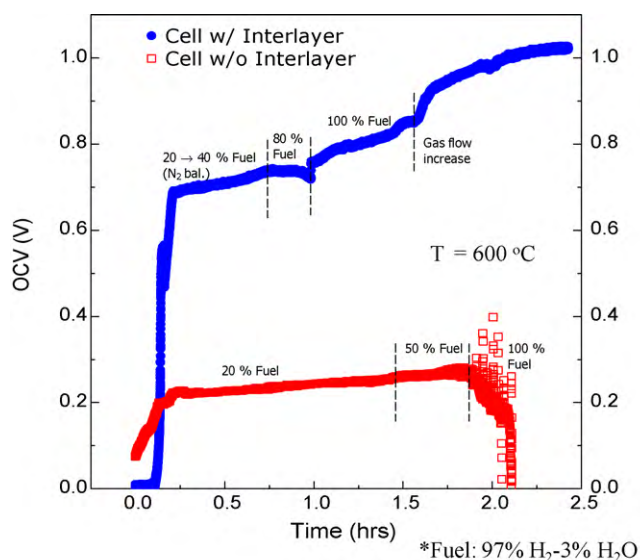
Fig. 6. OCV development in the thin film (1 μm) YSZ electrolyte cells with and without nano-structured NiO–YSZ interlayer.

nano-structured thin film electrolyte formation. This is because that the nano-structured thin film electrolyte is generally fabricated at relatively low temperatures ($\leq \sim$700–800 °C); and the post-annealing at $T \geq 1000$ °C would destroy the nano-scale microstructure of the thin film electrolyte. This applies to the cases of the free-standing membrane thin film SOFCs where the electrodes are formed after the electrolyte membrane is exposed.[8] Even some substrate materials used in free standing membrane SOFCs can be destroyed at this high temperature.[5]

However, the uniform nano-porous structures shown in Fig. 3 open a novel possibility of using these as the surface conditioning layers of bulk supports with micron-scale microstructures, in order to realize very thin yet mechanically stable electrolytes for SOFCs. As was reviewed in our previous article,[2] realizing mechanically stable thin film electrolyte SOFC which can be operated at a low temperature regime is very challenging. Thin film electrolyte SOFCs realized in the form of the free-standing membrane[4–6,8,10] has a significant issue in the thermal-mechanical stability.[26] On the other hand, if bulk-processed supports are used to realize a supported thin film electrolyte SOFC design, a substantial thickness of the electrolyte ($\sim$10 μm) is required for obtaining properly functioning SOFCs[27] since the flaw at the thin electrolyte depends on the pore size of the substrate.[28] Therefore, if the surface of the bulk-processed support is modified to have homogeneous nano-porous structure as shown in Fig. 3 then it is possible to realize a thermo-mechanically stable supported thin film electrolyte structure.

For investigating integrity of the YSZ electrolyte over the nano-porous Ni-YSZ interlayer, we fabricated a 2 cm by 2 cm cell with lanthanum strontium cobalt oxide (LSC) cathodes by PLD over thin PLD deposited YSZ electrolyte to observe the OCV development. For a comparison purpose, thin YSZ was deposited directly on the tape casted anode support without
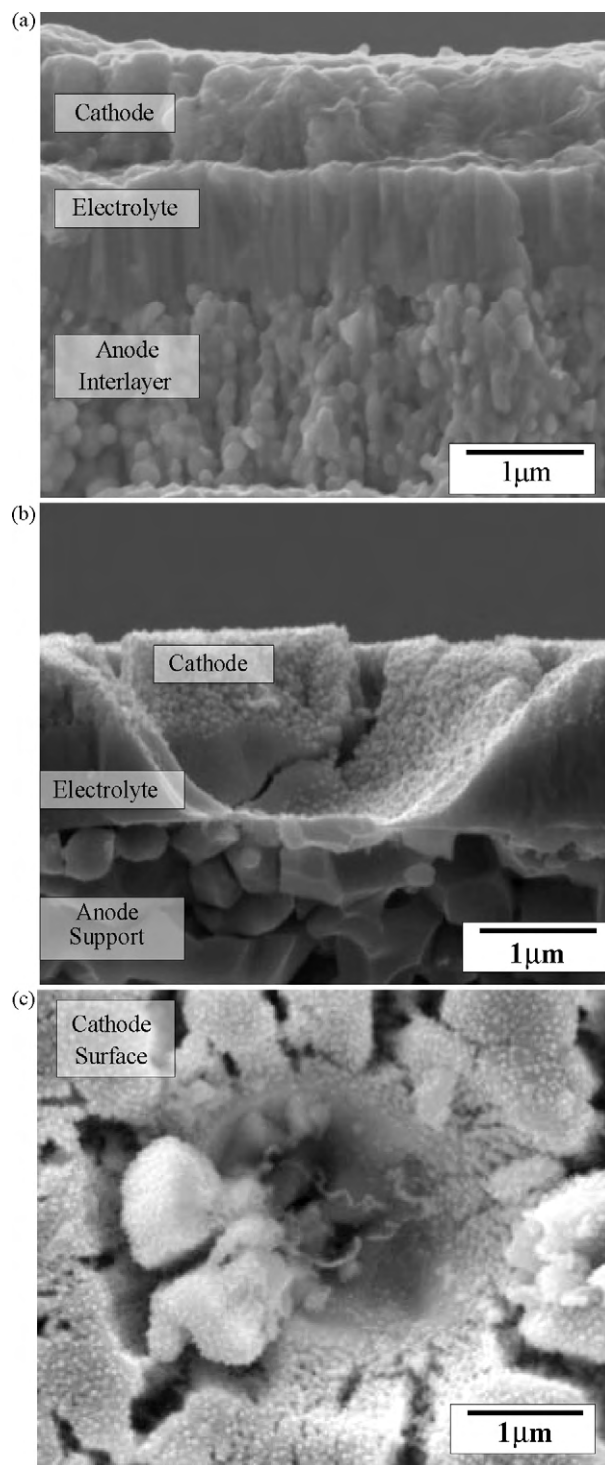


Fig. 7. (a) Cross-sectional microstructure of thin film electrolyte over nano-structured anode interlayer; (b) cross-sectional microstructure of a flaw showing rupture of thin film electrolyte; and (c) top-view of a flaw showing rupture of electrolyte.

the PLD NiO–YSZ interlayer. In Fig. 6, the OCV development difference during the reduction at 600 °C is shown. The OCV development was measured while reducing the anode by increasing the fuel (97% $H_2$–3% $H_2O$) percentage ($N_2$ balance) at the fuel side gradually while the cathode side was supplied with 100% air. The total gas flow rates at both the fuel and

air sides were 100 sccm. OCV over 1 V (1.034 V) was successfully obtained with the cell having the PLD NiO–YSZ interlayer between the thin electrolyte and the anode support.

Compared with that of other thin film membrane cells based on only PVD deposited thin film electrolytes,[4–6,10] the OCV value is fairly high and stable. The thin film electrolyte cells based on the nano-structure Ni-YSZ interlayer exhibited higher cell performances at low operating temperatures ($P_{max} = 145$ mW/cm$^2$ at 500 °C) when compared with those of other YSZ thin film electrolyte based cells with a comparable electrolyte thickness[5]; and no cell failure was observed more than 60 h of testing.[2] On the contrary, a very low OCV value was observed in the other cell (no interlayer) at the initial stage of the reduction then complete loss of the OCV value was resulted when 100% fuel was supplied to the anode side.

Microstructures of the cells after the cell operation are compared in Fig. 7. Fig. 7(a) shows a cross-sectional micrograph of the thin film electrolyte cell with the anode interlayer. The 1-μm thick electrolyte appears to have sustained its integrity well even after the operation lasted more than 60 h at 600 °C. On the contrary, the cell that exhibited the OCV drop in Fig. 6 (thin electrolyte directly deposited over the bulk anode support) contains substantial flaws. In Fig. 7(b) and (c), typical flaws observed in the cell without the interlayer are shown. Similar flaws with various sizes over micrometers showing destructions of the electrolyte are observed all over the cell. As mentioned previously, the flaw of the thin electrolyte fabricated on the support is significantly affected by the pore size of the support,[28] i.e., if the pore size of the support is bigger than the electrolyte thickness then pore induced flaws such as through pinholes or ruptures of the electrolyte originate. The bulk process anode support has micrometer sized pores thus only 1-μm thick electrolyte cannot sustain its microstructural integrity. The flaws such as Fig. 7(b) and (c) are where massive fuel and air intermixing occurs and the cause of the abrupt OCV drop.

From the result, we could conclude that the nano-structured Ni- and NiO–YSZ which is microstructurally stabilized by post-annealing is remarkably effective for mechanically supporting a thin film electrolyte in SOFCs. This approach has been proven to be a powerful method to obtain a supported thin film electrolyte structure in SOFCs, which exhibited improved low-temperature performances and better thermo-mechanical stability.[2]

## 4. Conclusions

The microstructural stability of the Ni-YSZ nano-composite obtained by the reduction of the PLD deposited NiO–YSZ thin film with variables such as post-annealing temperatures and reduction conditions has been studied. Grain growth by post-annealing of PLD NiO–YSZ films appears to be necessary to suppress Ni agglomeration in the Ni-YSZ nano-composite. The uniform nano-porous structure was very effective to obtain a supported thin film electrolyte structure in SOFCs. By employing the Ni-YSZ nano-porous interlayer, we could obtain a structurally stable 1-μm thick YSZ electrolyte over a porous support showing OCV higher than 1 V. The nano-structured interlayer

would play an important role in realizing thin film electrolyte SOFCs with high thermo-mechanical reliability.

## References

1. Noh H, Park J, Son J, Lee H, Lee J, Lee H. Physical and microstructural properties of NiO- and Ni-YSZ composite thin films fabricated by pulsed laser deposition at $T \leq 700$ °C. *J Am Ceram Soc* 2009;**92**(12):3064–9.
2. Noh H, Son J, Lee H, Song H, Lee H, Lee J. Low-temperature performance improvement of SOFC with thin film electrolyte and electrodes fabricated by pulsed laser deposition. *J Electrochem Soc* 2009;**156**(12):B1484–90.
3. Kim S, Son J, Lee K, Kim H, Kim H, Lee H, et al. Substrate effect on the electrical properties of sputtered YSZ thin films for co-planar SOFC applications. *J Electroceramics* 2010;**24**(3):153–60.
4. Bieberle-Hutter A, Beckel D, Infortuna A, Muecke UP, Rupp JLM, Gauckler LJ, et al. A micro-solid oxide fuel cell system as battery replacement. *J Power Sources* 2008;**177**:123–30.
5. Evans A, Bieberle-Hutter A, Rupp JLM, Gauckler LJ. Review on micro-fabricated micro-solid oxide fuel cell membranes. *J Power Sources* 2009;**194**:119–29.
6. Ignatiev A, Chen X, Wu N, Lu Z, Smith L. Nanostructured thin solid oxide fuel cells with high power density. *Dalton Trans* 2008;**40**:5501–6.
7. Litzelman SJ, Hertz JL, Jung W, Tuller HL. Opportunities and challenges in materials development for thin film solid oxide fuel cells. *Fuel Cells* 2008;**8**:294–302.
8. Huang H, Nakamura M, Su PC, Fasching R, Saito Y, Prinz FB. High-performance ultrathin solid oxide fuel cells for low-temperature operation. *J Electrochem Soc* 2007;**154**(1):B20–4.
9. Steele BCH, Heinzel A. Materials for fuel-cell technologies. *Nature* 2001;**414**:345–52.
10. Muecke UP, Beckel D, Bernard A, Bieberle-Hutter A, Graf S, Infortuna A, et al. Micro solid oxide fuel cells on glass ceramic substrates. *Adv Funct Mater* 2008;**18**:3158–68.
11. Fleig J, Tuller HL, Maier J. Electrodes and electrolytes in micro-SOFCs: a discussion of geometrical constraints. *Solid State Ionics* 2004;**174**(1–4):261–70.
12. Wang XH, Huang H, Holme T, Tian X, Prinz FB. Thermal stabilities of nanoporous metallic electrodes at elevated temperatures. *J Power Sources* 2008;**175**(1):75–81.
13. Muecke UP, Graf S, Rhyner U, Gauckler LJ. Microstructure and electrical conductivity of nanocrystalline nickel- and nickel oxide/gadolinia-doped ceria thin films. *Acta Mater* 2008;**56**(4):677–87.
14. Muecke UP, Akiba K, Infortuna A, Salkus T, Stus NV, Gauckler LJ. Electrochemical performance of nanocrystalline nickel/gadolinia-doped ceria thin film anodes for solid oxide fuel cells. *Solid State Ionics* 2008;**178**(33–34):1762–8.
15. Jou S, Wu T. Thin porous Ni-YSZ films as anodes for a solid oxide fuel cell. *J Phys Chem Solids* 2008;**69**:2804–12.
16. Jou S, Yeh D, Tseng A. Nickel nanorods produced by annealing composite oxide films. *J Nanosci Nanotech* 2008;**8**:390–2.
17. Tsai T, Barnett SA. Sputter deposition of cermet fuel electrodes for solid oxide fuel cells. *J Vac Sci Technol A* 1995;**13**(3):1073–7.
18. Wang LS, Barnett SA. Deposition, structure, and properties of cermet thin film composed of Ag and Y-stabilized zirconia. *J Electrochem Soc* 1992;**139**(4):1134–40.
19. La O, G J, Tuller HL, Shao-Horn Y. Microstructural features of RF-sputtered SOFC anode and electrolyte materials. *J Electroceramics* 2004;**13**(1–3):691–5.
20. Hayashi K, Yamamoto O, Nishigaki Y, Ninoura H. Sputtered Ni-Yttria stabilized zirconia composite film electrodes for SOFC. *Denki Kagaku* 1996;**64**(10):1097–101.

21. Wang LS, Barnett SA. Ag-perovskite cermets for thin film solid oxide fuel cell air-electrode applications. *Solid State Ionics* 1995;**76**: 103–13.

22. Hertz JL, Tuller HL. Nanocomposite platium-yttria stabilized zirconia electrode and implications for micro-SOFC operation. *J Electrochem Soc* 2007;**154**(4):B413–8.

23. Atkinson A, Barnett S, Gorte RJ, Irvine JTS, McEvoy AJ, Mogensen M, et al. Advanced anodes for high-temperature fuel cells. *Nat Mater* 2004;**3**:17–27.

24. Noh H, Son J, Lee H, Park J, Lee H, Lee J, Direct applicability of $La_{0.6}Sr_{0.4}CoO_{3-d}$ thin film cathode to yttria stabilized zirconia electrolytes at $T \leq 650 °C$. *Fuel Cells*, doi:10.1002/fuce.201000009.

25. Han J, Kim D. Analysis of the proportionality constant correlating the mean intercept length to the average grain size. *Acta Metall Mater* 1995;**43**(8):3185–8.

26. Baertsch CD, Jensen KF, Hertz JL, Tuller HL, Vengallatore ST, Spearing SM, et al. Fabrication and structural characterization of self-supporting electrolyte membranes for a micro solid-oxide fuel cell. *J Mater Res* 2004;**19**(9):2604–15.

27. Hobein B, Tietz F, Stover D, Cekada M, Panjan P. DC sputtering of yttria-stabilised zirconia films for solid oxide fuel cell applications. *J Eur Ceram Soc* 2001;**21**:1843–6.

28. DeJonghe LC, Jacobson CP, Visco SJ. Supported electrolyte thin film synthesis of solid oxide fuel cells. *Ann Rev Mater Res* 2003;**33**:169–82.